Journal of Inorganic Biochemistry 195 (2019) 83–90

Contents lists available at ScienceDirect

Journal of Inorganic Biochemistry

journal homepage: www.elsevier.com/locate/jinorgbio

Antigiardiasic activity of Cu(II) coordination compounds: Redox imbalance and membrane damage after a short exposure time

Yadira Rufino-González[a,1], Martha Ponce-Macotela[a,1], Juan Carlos García-Ramos[c,1], Mario N. Martínez-Gordillo[a], Rodrigo Galindo-Murillo[d], Angelica González-Maciel[b], Rafael Reynoso-Robles[b], Araceli Tovar-Tovar[e], Marcos Flores-Alamo[e], Yanis Toledano-Magaña[c,*], Lena Ruiz-Azuara[e,*]

[a] Laboratorio de Parasitología Experimental, Instituto Nacional de Pediatría, SSA, Insurgentes Sur No. 3700-C, Ciudad de México C. P. 04530, Mexico
[b] Laboratorio de Morfología Celular y Tisular, Instituto Nacional de Pediatría, SSA, Insurgentes Sur No. 3700-C, Ciudad de México C. P. 04530, Mexico
[c] CONACYT - UNAM - Centro de Nanociencias y Nanotecnología, Km 107 Carretera Tijuana-Ensenada, Ensenada, B.C. C.P. 22860, Mexico
[d] College of Pharmacy, University of Utah, Skaggs Hall 201, Salt Lake City, UT 84112, United States
[e] Facultad de Química, Universidad Nacional Autónoma de México, Avenida Universidad 3000, C.P. 04510 Ciudad de México, Mexico

ARTICLE INFO

Keywords:
Giardia intestinalis
Cu(II) coordination compounds
Antigiardiasic activity
Membrane damage
Oxidative stress

ABSTRACT

Giardiasis is a widespread illness that affects inhabitants of underdeveloped countries, being children and seniors the highest risk population. The several adverse effects produced by current therapies besides its increasing ineffectiveness due to the appearance of resistant strains evidence the urgent need for new therapeutic approaches. We present the antigiardiasic effect of eight Cu(II) coordination compounds, which belong to the family Casiopeínas. Two of them, 4,7-diphenyl-1,10-phenanthroline(acetylacetonato)copper(II) nitrate (**CasIII-Ha**,36 μM) and 4,7-diphenyl-1,10-phenanthroline(glycinato)copper(II) nitrate (**CasI-gly**,36 μM) have shown the best antiproliferative effect in *Giardia intestinalis* trophozoite cultures, both with the higher lipophilic character of the series. The antiproliferative effect of these coordination compounds is attributable to its capacity to interact with the cellular membrane and to increase reactive oxygen species (ROS) concentration within the parasite since the first hours of exposure, (2–6 h). We found that these compounds mainly induced the cell death of trophozoites by apoptosis, contrary to metronidazole, which induces apoptosis and necrosis in the same ratio. The cytotoxic effects on lymphocytes and macrophages isolated from human peripheral blood allowed us to establish a selectivity index and in turn, identify and propose the best candidates to continue with the assays in animal models. The selected molecules do not include the most active compounds against trophozoites, instead of that, we propose the compounds 4′,4′-dimethyl-2,2′-bipyridine(acetylacetonato)copper(II) nitrate (**CasIII-ia**,IC_{50} = 156 μM) and 4,7-dimethyl-1,10-phenanthroline(acetylacetonato) copper(II) nitrate (**CasIII-Ea**,IC_{50} = 125 μM), which possess an antiproliferative efficacy comparable with Metronidazole but also are those that produce the lowest effect on the viability of human lymphocytes and macrophages.

1. Introduction

Giardiasis is a “neglected disease” [1] that infects a population of 183.8 million, resulting in 171 thousand Disability Adjusted Life Years (DALYs) [2]. This zoonotic and re-emerging infectious disease [3] is an epidemic in developed countries and endemic in developing nations [4]. In Mexico, the *Giardia* seroprevalence is higher than 50% [5]. *Giardia intestinalis* (Syn. *G. lamblia, G. duodenalis*) cause abdominal pain, diarrhea, weight loss, and nutrient malabsorption, impairing the physical and mental development of children [6–8]. Antigiardiasic resistance is becoming a worldwide problem owing to the scarcity of new antiparasitic drugs [9], and the few commercially available are not 100% efficient [10].

Historically, quinacrine and furazolidone were the first drugs against *Giardia* [11]. The 5-nitroimidazoles such as metronidazole (Mtz) and tinidazole are the most common to treat giardiasis [12]. Benzimidazoles (albendazole and mebendazole) [13] and one nitrotiazol (nitazoxanide) also are other alternatives [14]. There are

* Corresponding authors.
E-mail addresses: yanistoledano@cnyn.unam.mx (Y. Toledano-Magaña), lenar701@gmail.com (L. Ruiz-Azuara).
[1] These authors contributed equally to this work.

https://doi.org/10.1016/j.jinorgbio.2019.03.012
Received 15 October 2018; Received in revised form 14 March 2019; Accepted 15 March 2019
Available online 21 March 2019
0162-0134/

several reports of meta-analysis comparing antigiardial drugs; nevertheless, results are controversial, owing to different efficacies between them [15,16]. All these chemical compounds produce undesirable secondary effects such as hyporexia, nausea, metallic taste, abdominal discomfort, vertigo, yellow skin and sclera, hemolysis, mutagenic and carcinogenic effects [10]. Besides, the *Giardia* evolution sooner or later will additionally select resistant strains [17], as is already being demonstrated with the nitroimidazoles [18]. With this panorama in mind, we found that parasites such as *Entamoeba histolytica*, *Trypanosoma cruzi, Plasmodium falciparum, Leishmania major* and several neoplastic cells share a common trait: they are sensitive to reactive oxygen species (ROS) which in turn give rise to apoptosis [19–24]. The search for compounds that generate the redox imbalance but whose adverse effects will be smaller than those produced by the compounds currently used in therapy has focused the attention of research groups to incorporate essential metals, particularly the use of Cu(II). A particular example of these Cu(II) coordination compounds is Casiopeínas, who have shown anticancer [25–27], antibacterial [28] and antiparasitic [29] activity through the generation of ROS. Due to all these results, we determine the growth inhibition capacity of eight Cu(II) coordination compounds belonging to the family of Casiopeínas over *G. intestinalis* trophozoite cultures. Also, explore the factors that trigger the apoptotic pathway on the exposed trophozoites. Besides, the selectivity indexes of these compounds through the cytotoxic tests on human peripheral blood lymphocytes and macrophages were determined.

2. Results and discussion

2.1. Synthesis and characterization of Cu(II) compounds

Cu(II) coordination compounds were synthesized as previously described in patents [30,31]. Elemental analysis, infrared (IR) and ultraviolet-visible (UV–Vis) spectroscopy, electron paramagnetic resonance (EPR), magnetic moment and conductivity measurements were performed to characterize the batch of compounds used in this work. All data agree with previously reported [32,33]. Scheme 1 shows the general structures of compounds studied in this work.

Fig. 1 shows the molecular structure of one of the most active compounds against *Giardia intestinalis* trophozoites, **Cas III-Ha** ([Cu (4,7-diphenyl-1,10-phenanthroline)(acetylacetonato)(H_2O)]NO_3). This compound presents a typical distorted square based pyramidal geometry [33] with tetrahedral distortion index (τ) of 0.074, where Cu(II) ion is slightly displaced out (0.1457 Å) of the main plane constituted by the nitrogen atoms of phenanthroline and the oxygen atoms of acetylacetonate. A water molecule occupies the apical position, and a nitrate ion acts as a counter ion. The supplementary information (SI; Tables S1 and S2), contains a detailed description of collection data and refining method besides the tables containing selected bond lengths and angles.

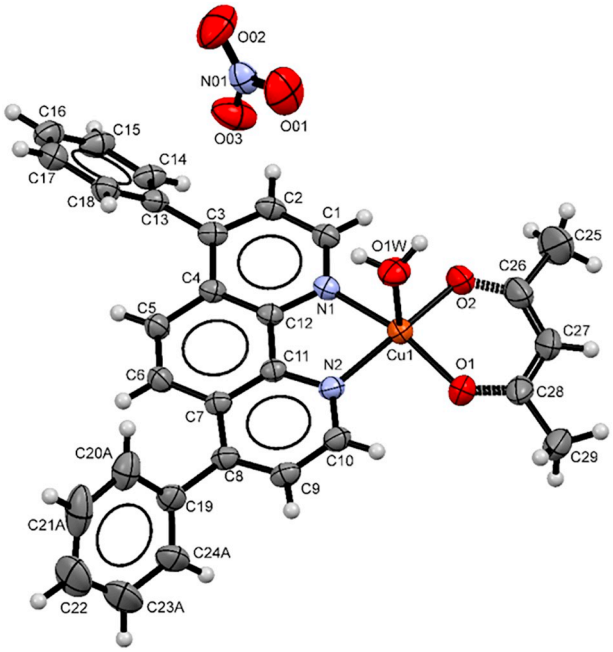

Fig. 1. ORTEP drawing (50% probability) for **CasIII-Ha**. [Cu (4, 7-diphenyl-1,10-phenanthroline) (acetylacetonato)] NO_3. Selected bond distances (Å): Cu1-N1 1.993(2), Cu1-N2 2.001(2), Cu1-O1 1.908(2), Cu1-O2 1.917(2), Cu1-O1w = 2.278(2). Selected bond angles (deg): O1-Cu1-N1 165.38(9), O2-Cu1-N1 93.20(9), O1-Cu1-N2 90.00(9), O2-Cu1-N2 169.86(9), N1-Cu1-N2 81.31(9), O1-Cu1-O1W 99.08(9), O2-Cu1-O1W 97.37(10).

2.2. Antigiardiasic activity

The eight coordination compounds employed in this work were chosen since they show moderate to high antiproliferative activity in several human tumor cell lines, producing this effect through apoptosis induction triggered by ROS production [22,23,26,27].

The antigiardiasic activity of these compounds was determined by the exposure of *G. intestinalis* trophozoites in vitro to different concentrations of the corresponding compound during 24 h. Then, the trophozoites that survived were washed and re-cultured in fresh media without treatment for other 24 h. After that, cell counting was

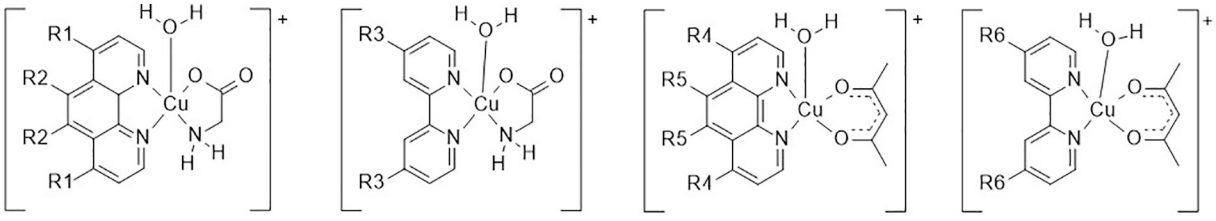

Cas Igly: R1=Ph, R2= H
Cas IIgly: R1=Me, R2= H
Cas VIgly:R1=H, R2= Me

Cas IV-gly: R3= Me

Cas III-Ha: R4=Ph, R5= H
Cas III-Ea: R4=Me, R5= H
Cas III-La: R4=H, R5= Me

Cas III-ia: R6=Me

Scheme 1. General structures of Cu(II) compounds studied in this work. Cas I-gly: Aqua(4,7-diphenyl-1,10-phenanthroline)(glycinato)copper(II) nitrate; Cas II-gly: Aqua(4,7-dimethyl-1,10-phenanthroline)(glycinato)copper(II) nitrate; Cas VI-gly: Aqua(5,6-dimethyl-1,10-phenanthroline)(glycinato)copper(II) nitrate; Cas IV-gly: Aqua(4,4′-dimethyl-1,10-phenanthroline)(glycinato)copper(II) nitrate; Cas III-Ha: Aqua(4,7-diphenyl-1,10-phenanthroline)(acetylacetonato)copper(II) nitrate; Cas III-Ea: Aqua(4,7-dimethyl-1,10-phenanthroline)(acetylacetonato)copper(II) nitrate; Cas III-La: Aqua(5,6-dimethyl-1,10-phenanthroline)(acetylacetonato)copper(II) nitrate; Cas III-ia: Aqua(4,4′-dimethyl-2,2′-bipyridine)(acetylacetonato)copper(II) nitrate.

Table 1
Cytotoxic effect of eight Cu(II) coordination compounds on *Giardia intestinalis* trophozoites, human peripheral blood lymphocytes (HPBL) and human peripheral blood macrophages (HPBM) cultures, their associated selectivity indexes, half-wave potential values vs. normal hydrogen electrode (NHE) and partition coefficient (LogP).

	G. intestinalis	HPBL	HPBM	SIL[a]	SIM[b]	$E_{½}$[c]	LogP[d]
	IC_{50}(μM)	IC_{50}(μM)	IC_{50}(μM)			(V)	
Cas I-gly	36.0	134.0	358.0	3.7	9.9	0.426	4.48
Cas III-Ha	36.0	64.0	136.0	1.7	3.7	0.418	5.85
Cas II-gly	214.6	1720.0	1140.0	8.0	5.3	0.330	1.67
Cas III-Ea	125.0	3860.0	1830.0	30.8	14.6	0.322	3.04
Cas III-La	126.5	35.0	1600.0	0.2	12.6	0.342	3.04
Cas VI-gly	188.6	216.0	3800.0	1.1	20.1	0.348	2.54
Cas III-ia	156.0	4700.0	2470.0	30.1	15.8	0.302	1.17
Cas IV-gly	233.5	3260.0	14,600.0	13.9	62.5	0.324	1.67
Mtz	119.7	> 100				−1.01	0.05

[a] Selectivity Index Lymphocytes (SIL) = IC_{50} HPBL/IC_{50} *Giardia* trophozoites
[b] Selectivity Index Macrophages (SIM) = IC_{50} HPBM/IC50 *Giardia* trophozoites.
[c] $E_{½}$(V) = Half-wave redox potential of coordination compounds taken from reference [32,33].
[d] logP = The value of Distribution coefficient given for each compound was obtained by the addition of non-coordinated ligands values without considering Cu(II) ion (ΣlogP). Data were taken from the ChemSpider database. www.chemspider.comConsulted 07/02/2018.

performed to determine the corresponding half-inhibitory concentration (IC_{50}).

Results are compiled in Table 1 and show that only two compounds present significant effectiveness to inhibit the proliferation of *Giardia intestinalis* trophozoites than metronidazole (**Mtz**), **Cas-Igly** and **Cas III-Ha,** both with an IC_{50} value of 36.0 μM. The rest of the compounds present comparable or lower inhibition potency compared with **Mtz**.

Thus, the antigiardiasic activity of these compounds follows the order: **CasI-gly** ~ **CasIII-Ha** > **Metronidazole** > **CasIII-Ea** > **CasIII-La** > **CasIII-ia** > **CasVI-gly** > **CasII-gly** > **CasIV-gly**. Interestingly, the most active compounds in this work are also the most hydrophobic of the series. In a general way, as the lipophilic character decreases (Table 1), the inhibition potency decreases (higher IC_{50} values). In this case, compounds with acetylacetonate in the coordination sphere of Cu(II) ion are the most actives, except for **Cas I-gly**, for which the lipophilic character is dictated by the diphenylated-phenanthroline and masks the contribution of the second ligand.

As established previously by our group, the lipophilic/hydrophilic character of these metal complexes can be very well described using the sum of the values corresponding to the log P of the ligands in its non-coordinated form (Table 1) [32]. Thus, Fig. 2 shows the dependence of *Giardia intestinalis* viability with the redox potential and the theoretical partition coefficient of Cu(II) coordination compounds.

Differentiating two groups of compounds on each graph is possible. Both, the redox potential and the theoretical partition coefficient, present an inverse relationship with the trophozoites viability. Which means that the antigiardiasic activity increases as the redox potential becomes more positive or when the lipophilic character increases. Eqs. (1)–(4) describe each behavior.

$$-\log\left(\frac{1}{IC_{50}}\right) = 4.51455–6.56401\ E^{gly}_{1/2};\ r^2 = 0.985 \quad (1)$$

$$-\log\left(\frac{1}{IC_{50}}\right) = 3.9246–5.9953\ E^{acac}_{1/2};\ r^2 = 0.931 \quad (2)$$

$$-\log\left(\frac{1}{IC_{50}}\right) = 2.11648–0.20457\ \sum_{gly} logP;\ r^2 = 0.990 \quad (3)$$

$$-\log\left(\frac{1}{IC_{50}}\right) = 2.11648–0.20457\ \sum_{acac} logP;\ r^2 = 0.999 \quad (4)$$

The same descriptors than the used in the above equations are very useful to describe the antiproliferative activity of Casiopeínas against human tumor cell lines, but in that case, the lipophilic character only has a small contribution. The proposed mechanism of action for the antiproliferative activity of Casiopeínas on tumor cells are ROS overproduction and DNA interaction. Both, independently or concomitantly, produce irreversible cell damage that leads cells to apoptosis [22,23,34–37]. The reaction of the metal compound with glutathione (GSH) in the presence of molecular oxygen or hydrogen peroxide generates superoxide and hydroxyl radical overproduction within the cell [22,23,27,34,37]. On the other hand, DNA interaction is through minor groove binding [35,38].

Due to the above findings and to explore the pathways that produce the death of the parasite, we looked for morphological changes in treated trophozoites by optical and electronic microscopy, and the presence of apoptosis markers and ROS production by flow cytometry.

Apoptotic-like features have been described for programmed cell death of several unicellular eukaryotes [39]. For *G. intestinalis* these features involve cell shrinkage, chromatin condensation, membrane blebbing and vacuolization. Optical (data not shown) and transmission electron microscopy (TEM) were used to evidence the morphological changes (Fig. 3). After 24 h of exposure to the IC_{50} values found for compounds **Cas I-gly**, **Cas III-Ha** and **Mtz** the electronic microscopy images were acquired. Fig. 3a shows cytoplasmic and nuclear membrane integrity of untreated trophozoites with the characteristic electron-dense appearance due to the presence of cytoplasmic glycogen

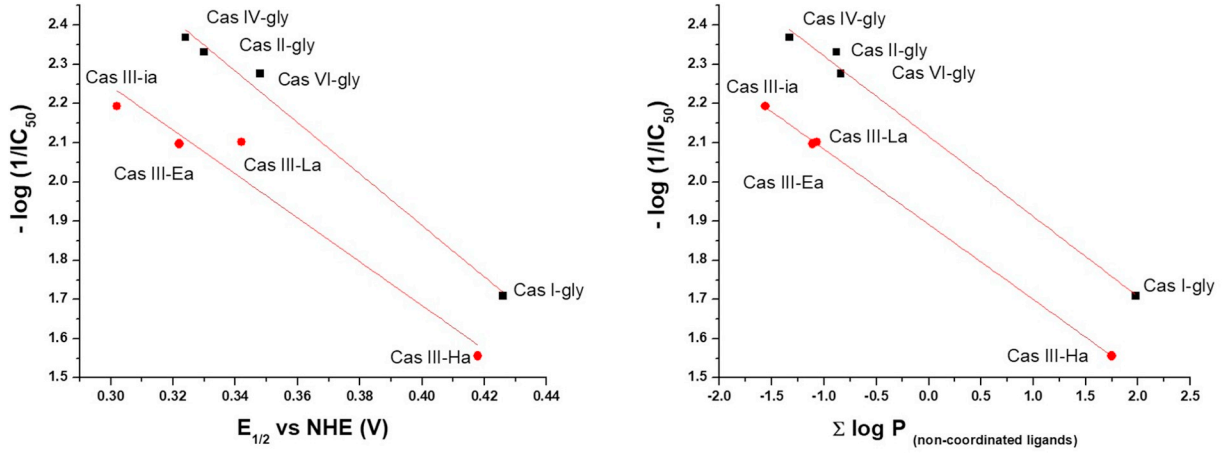

Fig. 2. Dependence of *Giardia intestinalis* trophozoites viability with a) the redox potential and b) the lipophilic character.

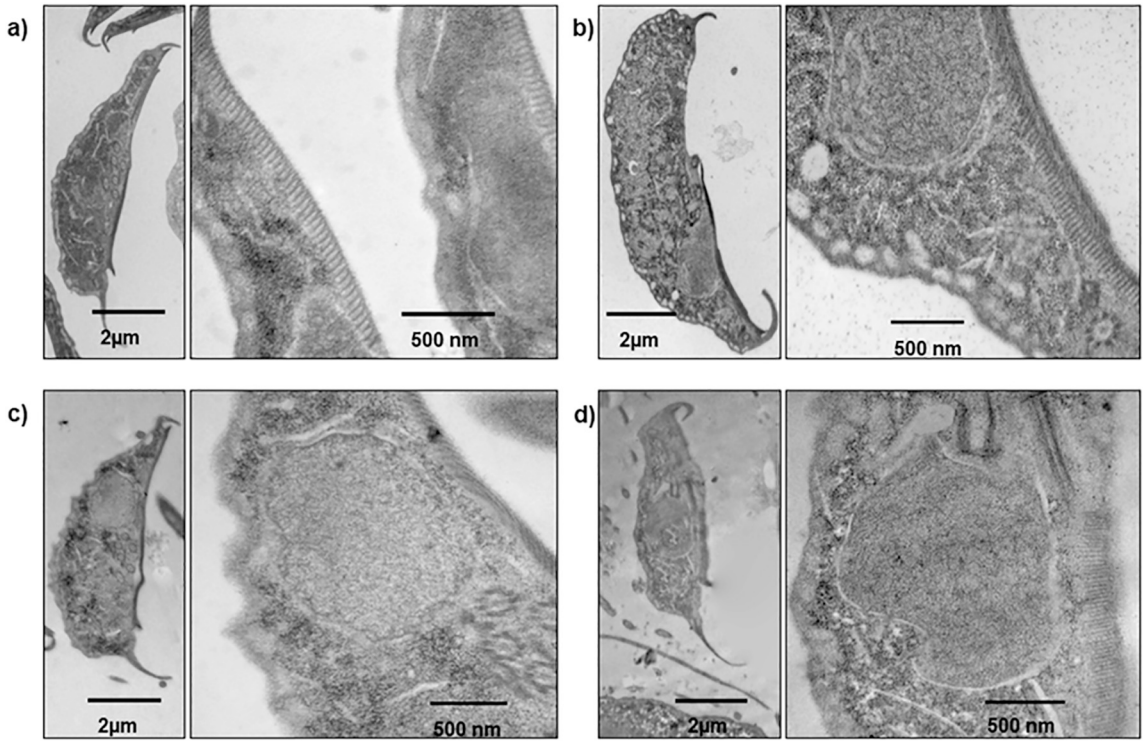

Fig. 3. TEM images showing the morphological changes on *G. intestinalis* trophozoites produced by the 24 h exposure to the IC_{50} values of the evaluated compounds compared with those without treatment. a) **Control**, b) **Mtz**, c) **CasI-gly** and d) **CasIII-Ha**.

granules and ribosomes. Also presents distinctive features such as peripheral vacuoles, endoplasmic reticulum cisternae and the well-defined structure for the lateral crest and adhesive disk.

Trophozoites treated with **Mtz** (Fig. 3b) shown a decrease in the electron-dense appearance, fragmentation of the double-nuclear membrane and in some places of the adhesion disk. Besides, vacuoles near the perinuclear cisternae and endoplasmic reticulum cisternae appears, which is evidence of increased metabolic activity, probably due to the detoxification processes intensification activated by the parasite.

On the other hand, trophozoites treated with **Cas I-gly** (Fig. 3c) and **Cas III-Ha** (Fig. 3d) show cellular size increase. Also, it is clear the lack of nuclear as well as membranes that limit the dorsal and cytoplasmic vacuoles. We observe completely destroyed basal bodies, and there is acute damage to some regions of the adhesive disk. In both treatments, it is possible to identify sizeable endoplasmic reticulum cisternae in the trophozoites, suggesting a metabolic response increased. Additionally, is observed damage on axonemes in trophozoites treated with **Cas III-Ha**.

The appearance of endoplasmic reticulum cisternae either in **Mtz** or Casiopeínas treatments suggests a common feature of damage production. The principal mechanism of action for the antiproliferative activity of **Mtz** is ROS production. Thus, we explore the capacity of these three compounds (**Mtz**, **CasIII-Ha**, and **CasI-gly**) to produce it. Besides, we determined the cell death pathway induced (apoptosis or necrosis) and changes in cellular size (Fig. 4). Flow cytometry dot plots for all treatments can be consulted in the SI Fig. S1 and S2.

Effectively, coordination compounds increase ROS concentration within trophozoites, faster and about 5-fold more efficiently than **Mtz** does at the first evaluated times. It seems that the rapid increase of ROS concentration observed is inversely related to trophozoites viability. **CasIII-Ha** produces the highest changes in ROS concentration at 2 and 6 h of exposure and promotes the most significant differences in viability at these exposure times (Fig. 3a and b). It could be possible that the increase in the first hours led to a 90% decrease in viability of trophozoites treated with both Casiopeínas, compared to 50% observed with **Mtz** at 24 h (Fig. 4a).

Thus, the redox potential of coordination compounds seems to be useful to explain the viability difference between **Cas III-Ha** and **Cas I-gly**; however, it is not enough to justify the general trend where the antiproliferative potency increases as their lipophilic character do.

Looking for further details, we found that **Cas I-gly** produces cell size increase in almost 60% of cells after 2 h of exposure, but with time, cell size returns to average values. We observe something similar for **Cas III-Ha** but at longer exposure times (6 h) and only with half of the cells (30%) (Fig. 4c). Cell size increase must be related to the effortless passing through the cellular membrane, due to the significant changes were produced by the most hydrophobic compound (Table 1).

To explore this hypothesis, we performed a Molecular Dynamics (MD) simulations to study the interaction between these Casiopeínas and dioleoylphosphatidylcholine (DOPC) membrane model. Recently, this model was useful to describe the differential toxicity of two Casiopeínas in blood peripheral human lymphocytes [40]. Fig. 4 shows the energy profile of the copper-compounds as they diffuse through a membrane. The potential of mean force profile is almost identical for both compounds (Fig. 5). The energy required to stabilize them in the layer is 41.47 Kcal/mol and 40.11 Kcal/mol for **Cas III-Ha** and **Cas I-gly**, respectively. Both compounds have reached the energy minimum at ~26.5 Å within the glycerol and the aliphatic chain of the DOPC monomers. From the above results, it seems that the non-aromatic ligand hardly contributes to Cu (II) compounds cross the cell membrane, despite that they provoke significant differences in Log *P* values according to Table 1. Therefore, this indicates that phenanthroline strongly modulates the passage through the membrane. A fine-tune modulation is provided either by the substituent of the diimine and by the secondary ligand, in this case, glycinate or acetylacetonate. As expected, energetic differences between both compounds are minimal but, as we have shown in previous works with these compounds, these small differences are just enough to explain their different reactivity and their biological effects [40]. Thus, the MD simulation of the diffusion through the membrane model suggest that the cellular membrane could more retain **Cas I-gly** than **Cas III-Ha**.

According to these results, the antigiardiasic activity of Casiopeínas

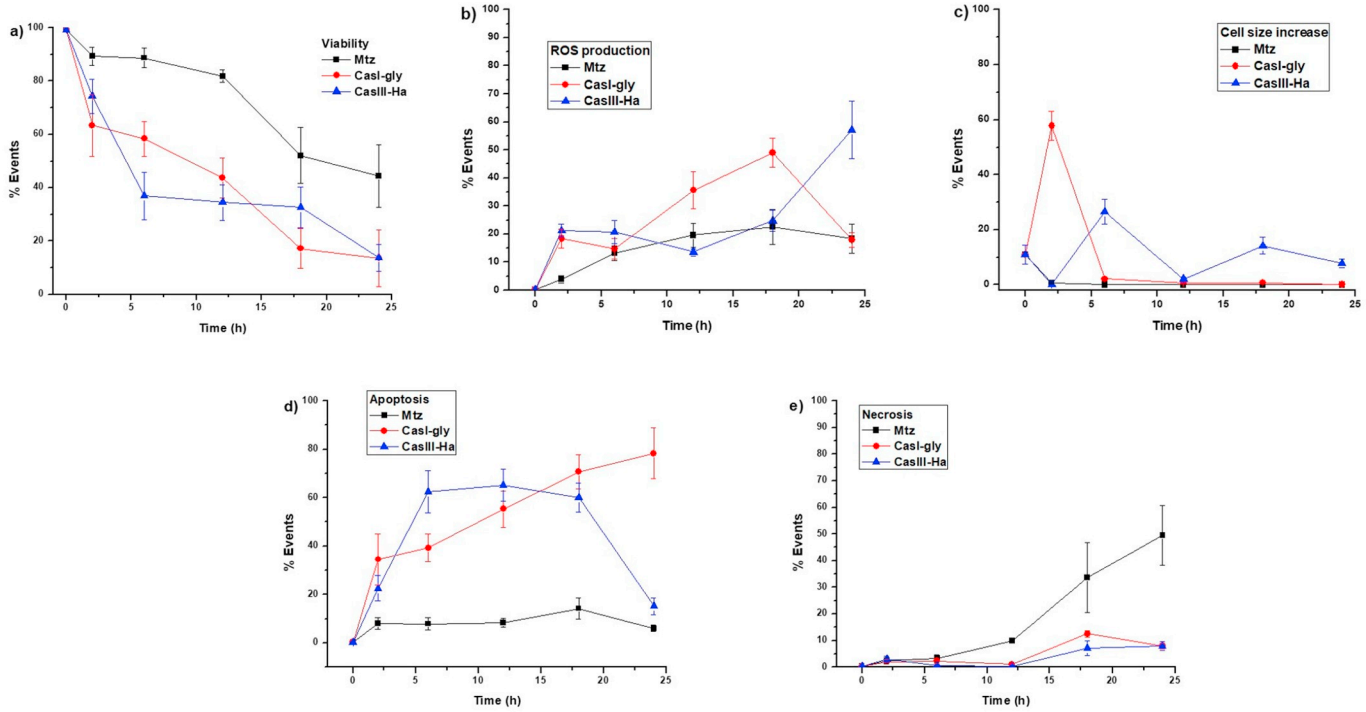

Fig. 4. Cellular parameters assessed by flow cytometry in *Giardia intestinalis* trophozoites after 2, 6, 12, 18 and 24 h of exposure to IC_{50} of **Mtz** (119.7 μM), **Cas III-Ha** (36.0 μM) and **Cas I-gly** (36.0 μM). a) Viability; b) Changes in ROS concentration; c) Modifications in cell size during the exposure; d) Apoptosis and e) Necrosis.

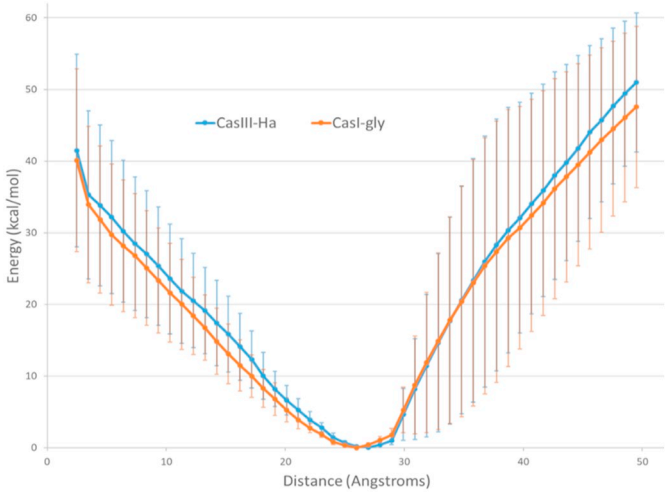

Fig. 5. PMF energy profile (kcal/mol) for copper compounds **Cas III-Ha** (blue line) and **Cas I-gly** (gold line). The x-axis is the distance (Å) from the center of mass of the lipid bilayer membrane and the center of mass of the compound. Error bars show ± standard deviation.

is strongly related to their retention in the cellular membrane and their capacity to participate in redox reactions. On the trophozoites, it is quite possible that one of the primary targets of Casiopeínas will be the enzyme pyruvate-ferredoxin oxidoreductase (PFOR), which besides the thiols, can participate as a reducing agent for the redox transformation Cu(II)/C(I) of the metal compounds. This enzyme possesses three 4Fe−4S units [41] with a redox potential of −0.5 V vs. NHE [42]. Luminal protozoa and bacteria share PFOR, and it is responsible for reducing the ferredoxin or flavodoxin which in turn transfers an electron to **Mtz** to activate it [43].

As mentioned earlier, Casiopeínas produce more and faster ROS than **Mtz**. Most antiproliferative agents are also the best oxidizing agents. Thus, PFOR (−0.5 V vs. NHE) could reduce Cu(II) compounds (0.3 to 0.425 V vs. NHE; Fig. 2) which in turn could react with several biomolecules producing the redox unbalance. Generated ROS could be then, responsible for triggering the apoptotic response of the parasites leading to its death.

Giardia's PFOR is a membrane-associated enzyme and with a limited cytosolic presence [44]. Thus, if the redox reaction previously described occurs in the membrane, this could explain cellular size increment, highest levels of ROS and the highest percentage of apoptotic cells after short exposure times. Also, could clarify that after 24 h, apoptosis in **Cas III-Ha** abruptly decreases, probably regulated by the cytosolic antioxidant response, while apoptosis continues increasing for the compound that could be more retained in the cellular membrane, **Cas I-gly**.

All damages observed on trophozoites treated with Casiopeínas allow us to suggest that are produced so quickly that avoids the parasite response to stress, even when parasite tries to respond through the increase of its metabolic activity. Also, it allows us to encourage other research groups to assess, when possible, their determinations of cell viability parameters at short exposure times and obtain more information regarding the effects of their candidate molecules.

It is important to note that neither **Cas I-gly** nor **Cas III-Ha** induce > 13% of necrosis in all assessed times. We observe the opposite behavior for **Mtz**, for which the necrosis reached 50% after 24 h of exposure.

Regarding cell death induced pathways, the effects for healthy cells and considering the possible use of these compounds in the treatment of disease, we have determined the impact over first-line response cells in the human body such as human peripheral blood lymphocytes (HPBL) and macrophages (HPBM). We evaluate the effect of Casiopeínas in HPBL and HPBM cultures to achieve this goal. Values found are reported as IC_{50} values in Table 1.

The equation Selectivity Index = (IC_{50} mammalian cells)/(IC_{50} trophozoites) was used to calculate a selectivity index. Selectivity index is within the ranges 0.27 to 30.88 in HPBL and 3.77 to 62.52 for HPBM. As expected, the most potent growth inhibiting compounds on trophozoites cultures are also some of the most cytotoxic compounds for human lymphocytes and macrophages, that is, **Cas I-gly** and **Cas III-Ha**. The selectivity index of these compounds is 3.72 and 1.77 on HBPL

and 9.93 and 3.37 for HBPM, respectively.

Despite their effectiveness inhibiting the trophozoites growth, **Cas I-gly** and **Cas III-Ha** are highly cytotoxic to human lymphocytes and macrophages. Therefore, still decreasing its efficacy against trophozoites, it is essential to focus the efforts on those compounds with the highest selectivity index and who could produce the lowest adverse effects.

From Table 1, compounds that satisfy both requirements, antigiardiasic effects and the lower impact on human macrophages or lymphocytes viability are **Cas III-Ea** and **Cas III-ia**. An additional advantage of **Cas III-ia** is the existence of a complete preclinical dossier because nowadays is in Phase I Clinical trials as an anticancer agent. All this information background could accelerate the use of this compound as an alternative in the treatment of giardiasis. Therefore, it is imperative to continue the antigiardiasic assays on in vivo models, firstly of **Cas III-ia**, and closely followed by **Cas III-Ea**.

3. Conclusions

Our results show that Casiopeínas produce their antiproliferative effect on *Giardia intestinalis* trophozoites cultures by the interaction with the cellular membrane and their capacity to increase ROS concentration within the trophozoites, producing very significant damage to cells at very short exposure times. From very early exposure times, a large cell population presents apoptosis markers, being this the main death pathway exerted by these compounds, in contrast to metronidazole, which induces apoptosis and necrosis in the same ratio. Interaction of Casiopeínas with the cellular membrane seems to be a key factor for their antigiardiasic activity because they probably can react with the membrane-associated enzyme pyruvate-ferredoxin oxidoreductase (PFOR), an essential enzyme for the biotransformation of metronidazole, leading to the redox imbalance in the parasite responsible for the apoptosis pathway triggering.

Selectivity indexes allow us to identify potential candidates to complete its preclinical data; these compounds are **Cas III-ia** and **Cas III-Ea**. Being the former the principal candidate, because it already reached Phase I clinical trials as an anticancer agent. Thus, the usage of the **Cas III-ia** preclinical data could accelerate the employment of this compound now as an alternative to treat giardiasis. These results also open the way to explore either other members of the Casiopeínas family or other coordination compounds that possess suitable redox potential and lipophilic/hydrophilic character values as possible not only antigiardiasic but as broad-spectrum antiparasitic agents.

4. Experimental section

4.1. Synthesis and characterization

The following paragraphs compile the characterization of the batch of compounds used in this work. The characterization data agree with previous reports [32,33].

Cas I-gly [Cu(4,7-diphenyl-1,10-phenanthroline)(glycinato)(H_2O)]NO_3 Elemental analysis (%) calculated for $CuC_{26}H_{23}N_4O_6$ (559.01 $gmol^{-1}$): C 55.81, H 4.11, N 10.01. Found: C 55.69, H 4.02, N 9.95. IR (KBr): ν = 3449, 3240, 1604, 1522, 1428, 1384 (NO_3), 852, 709, 622 cm^{-1}. UV/Vis (MeOH): λ_{max} (ε) = 604 nm (52 $M^{-1}cm^{-1}$). μ_{eff} = 1.85 BM. Λ (MeOH) = 71.5 Scm^2mol^{-1}. EPR (MeOH, 77 K): $g_\parallel$ = 2.275, $g_\perp$ = 2.035, $A_\parallel = 183.0 \times 10^{-4}\,cm^{-1}$, $A_\perp = 7.6 \times 10^{-4}\,cm^{-1}$.

Cas II-gly [Cu(4,7-dimethyl-1,10-phenanthroline)(glycinate)(H_2O)]NO_3. Elemental analysis (%) calculated for $CuC_{16}H_{20}N_4O_7$ (443.9 $gmol^{-1}$): C 43.29, H 4.54, N12.62. Found: C 43.53, H 4.70, N 12.61. IR (KBr): ν = 3446, 3255, 1602, 1525, 1429,1383 (NO_3), 871, 726, 637 cm^{-1}. UV (MeOH): λ_{max} (ε) = 623 nm (58 $M^{-1}cm^{-1}$). μ_{eff} = 1.76 BM. Λ (MeOH) = 75.1 Scm^2mol^{-1}. EPR (MeOH, 77 K) = $g_\parallel$ = 2.237, $g_\perp$ = 2.054, $A_\parallel = 189.0 \times 10^{-4}\,cm^{-1}$, $A_\perp = 7.6 \times 10^{-4}\,cm^{-1}$.

Cas VI-gly [Cu(5,6-dimethyl-1,10-phenanthroline)(glycinate)(H_2O)]NO_3 Elemental analysis (%) calculated for $CuC_{16}H_{16}N_4O_5{\cdot}0.5H_2O$ (416.86 $gmol^{-1}$): C 46.09, H 4.10, N 13.43. Found: C 46.11, H 4.21, N 13.43. IR (KBr): ν = 3421, 3261, 1632, 1525, 1435, 1385 (NO_3), 822, 709, 597 cm^{-1}; UV (MeOH): λ_{max} (ε) = 612 nm (60 $M^{-1}cm^{-1}$); μeff = 1.71 BM. Λ (MeOH) = 76.1 Scm^2mol^{-1}. EPR (MeOH, 77 K) = $g_\parallel$ = 2.242, $g_\perp$ = 2.056, $A_\parallel = 190.0 \times 10^{-4}\,cm^{-1}$, $A_\perp = 7.6 \times 10^{-4}\,cm^{-1}$.

Cas IV-gly [Cu(4,4′-dimethyl-2,2′-bipyridine)(glycinate)(H_2O)]NO_3. Elemental analysis calculated for $CuC_{14}H_{16}N_4O_6{\cdot}0.5H_2O$ (408.9 $gmol^{-1}$): C 41.12, H 4.18, N13.70. Found: C 40.92, H 4.12, N 13.60. IR (KBr): ν = 3430, 3250, 1629,1519, 1426, 1384 (NO_3), 822, 722, 635 cm^{-1}. UV/Vis (MeOH): $\lambda_{max}(\varepsilon)$ = 624 nm (62 $M^{-1}cm^{-1}$). μ_{eff} = 1.74 BM. Λ (MeOH) = 87.9 Scm^2mol^{-1}. EPR (MeOH, 77 K) = $g_\parallel$ = 2.236, $g_\perp$ = 2.056, $A_\parallel = 191.0 \times 10^{-4}\,cm^{-1}$, $A_\perp = 7.6 \times 10^{-4}\,cm^{-1}$.

Cas III-Ea [Cu(4,7-dimethyl-1,10-phenanthroline)(acetylacetonate)(H_2O)]NO_3 Elemental analysis (%) calculated for $CuC_{19}H_{21}N_3O_6$ (450.9 $gmol^{-1}$): C 50.61, H 4.69, N 9.32. Found: C 50.32, H 4.55, N 9.21. IR (KBr): ν = 3413, 1622, 1577, 1521, 1425, 1384 (NO_3), 869, 725 cm^{-1}. UV/Vis (MeOH): λ_{max} (ε) = 608 nm (65 $M^{-1}cm^{-1}$). μ_{eff} = 1.80 BM. Λ (MeOH) = 87.0 Scm^2mol^{-1}. EPR (MeOH, 77 K) = $g_\parallel$ = 2.226, $g_\perp$ = 2.055, $A_\parallel = 182.0 \times 10^{-4}\,cm^{-1}$, $A_\perp = 8.0 \times 10^{-4}\,cm^{-1}$.

Cas III-Ha [Cu(4,7-diphenyl-1,10-phenanthroline)(acetylacetonate)(H_2O)]NO_3 Elemental analysis (%) calculated for $CuC_{29}H_{25}N_3O_6$ (575.0 $gmol^{-1}$): C 60.57, H 4.38, N 7.31. Found: C 60.43, H 4.22, N 7.22. IR (KBr): ν = 3417, 1620, 1585, 1517, 1427, 1384 (NO3), 854, 736 cm^{-1}. UV/Vis (MeOH): λ_{max} (ε) = 609 nm ($M^{-1}cm^{-1}$). μ_{eff} = 1.87 BM. Λ (MeOH) = 78.0 Scm^2mol^{-1}. EPR (MeOH, 77 K) = $g_\parallel$ = 2.221, $g_\perp$ = 2.059, $A_\parallel = 179.9 \times 10^{-4}\,cm^{-1}$, $A_\perp = 6.0 \times 10^{-4}\,cm^{-1}$.

Cas III-ia [Cu(4,4′-dimethyl-2,2′-bipyridine)(acetylacetonate)(H_2O)]NO_3. Elemental analysis calculated (%) for $CuC_{17}H_{21}N_3O_6$ (426.9 $gmol^{-1}$): C 47.83, H 4.96, N 9.84. Found: C 47.84, H 5.07, N 9.97. IR (KBr): ν = 3463, 1616, 1587, 1525, 1490, 1384, (NO_3), 730 cm^{-1}. UV/Vis (MeOH): λmax (ε) = 602 nm (58 $M^{-1}cm^{-1}$). μ_{eff} = 1.80 BM. Λ (MeOH) = 81.5 Scm^2mol^{-1}. EPR (MeOH, 77 K) = $g_\parallel$ = 2.221, $g_\perp$ = 2.056, $A_\parallel = 182.0 \times 10^{-4}\,cm^{-1}$, $A_\perp = 8.0 \times 10^{-4}\,cm^{-1}$.

Cas III-La [Cu(5,6-dimethyl-1,10-phenanthroline)(acetylacetonate)(H_2O)]NO_3 Elemental analysis for (%) $CuC_{19}H_{23}N_3O_7$ (468.9$gmol^{-1}$): C 48.66, H 4.94, N 8.96. Found: C 48.45, H 4.70, N 8.73. IR (KBr): ν = 3488, 1606, 1581, 1517, 1430, 1384 (NO_3), 819, 730 cm^{-1}. UV/Vis (MeOH): λmax (ε) = 604 nm (64 $M^{-1}cm^{-1}$). μ_{eff} = 1.82 BM. Λ(MeOH) = 80.0 Scm^2mol^{-1}. EPR (MeOH, 77 K) = $g_\parallel$ = 2.221, $g_\perp$ = 2.056, $A_\parallel = 178.5 \times 10^{-4}\,cm^{-1}$, $A_\perp = 8.0 \times 10^{-4}\,cm^{-1}$.

4.2. X-ray crystallographic structure determinations

Siemens P4 four-cycle diffractometer equipped with graphite-monochromatic the Mo-K_α radiation was used to perform the X-ray measurements of **CasIII-Ha** at 298 K, λ = 0.71073 Å, using a ω scan width of 1.60° and a variable scan rate of 4–30° min^{-1}. Structure solution and refinement were carried out with the SHELXS-2014 [45] and SHELXL-2014, [46] respectively; WinGX v2014.1 software was used to prepare material for publication [47]. Full-matrix least-squares refinement was carried out by minimizing $(Fo^2–Fc^2)^2$. All non-hydrogen atoms were refined anisotropically. H atoms of the water molecule (H—O) were located in a difference map and refined isotropically with Uiso(H) = 1.5 for H—O. H atoms attached to carbon were placed in geometrically idealized positions and refined as riding on their parent atoms, with C–H = 0.93–0.96 Å and with Uiso(H) = 1.2Ueq(C) for aromatic, and Uiso(H) = 1.5Ueq(C) for methyl groups. C20a C21a C23a C24a and C20b C21b C23b C24b are disordered over two sites with occupancies 0.5:0.5. Crystallographic data have been deposited at the Cambridge Crystallographic Data Center as supplementary material number CCDC 914789. Copies of the data can be obtained free of charge on application to CCDC, 12 Union Road, Cambridge CB2 1EZ, UK. *E*-Mail: deposit@ccdc.cam.ac.uk.

4.3. Giardia intestinalis trophozoite cultures

Giardia intestinalis trophozoites were incubated in TYI-S-33 medium until reaching log phase. Afterward, 5×10^4 trophozoites were exposed by 24 h at 37 °C to several concentrations (5.25–100 μg/ml) of **Cas I-gly**, **Cas II-gly**, **Cas IV-gly**, **Cas VI-gly**, **Cas III-Ea**, **Cas III-Ha**, **Cas III-ia,** and **Cas III-La**. After 24 h, the trophozoite cultures were cooled by 15 min and then centrifuged at 3500 rpm. Medium was removed and replaced by a fresh one without compounds. Finally, the cultures with new TYI-S-33 medium were incubated by other 24 h, then were cooled again and quantified using a Neubauer chamber. DMSO was used to dissolve Casiopeínas. As controls were used trophozoites without treatment, trophozoites with 0.05% of DMSO, and trophozoites exposed to 20 μg/ml of metronidazole. The group of trophozoites without treatment is considered as 100% of viability. Each determination was done in three independent experiments by triplicate. Viability, apoptosis/necrosis, and ROS quantification were performed by flow cytometry after 2, 6, 12, 18 and 24 h of exposure to the IC_{50} values of compounds **CasIgly, CasIIIHa,** and **Mtz**. All stains were used following the provider protocol. Cell viability was determined using the Vybrant™ CFDA-SE cell tracer kit and propidium iodide (PI) (Thermo Fisher Scientific V12883). Apoptosis and necrosis were assessed with the Alexa Fluor® 488 Annexin V/Dead Cell Apoptosis kit (Thermo Fisher Scientific V13241). Reactive oxygen species generation was analyzed with MitoSOX™ Red mitochondrial superoxide indicator for live-cell imaging (Invitrogen M36008). All determinations were performed in a BD FACS ARIA I flow cytometer.

4.4. Transmission electron microscopy (TEM)

G. intestinalis trophozoites from experimental and control groups were fixed in 2.5% glutaraldehyde buffered with phosphate buffer (0.1 M, pH 7.2), post-fixed in 1% osmium tetroxide, dehydrated in an ethanol series and embedded in epoxy resin (Epon) to identify ultrastructural modifications. Ultra-thin sections (60–90 nm) were cut and collected on slot grids covered with formvar membrane. Sections were stained with uranyl acetate and lead citrate. The structural changes from 50 fields for each sample were examined and recorded using a JEM-1011 (JEOL, Osaka, Japan) microscope.

4.5. Human peripheral blood lymphocytes and macrophages

Evaluation of the antiproliferative activity of coordination compounds in human peripheral blood lymphocytes and macrophages were performed following the procedures previously reported [22,40].

4.6. Computational chemistry

The structures of the copper complexes were extracted from X-ray crystal data and optimized by using the meta hybrid functional m06-2× with the 6–311 + + G(d,p) basis set. The DFT level of theory has previously been proven to reproduce experimental structures [35,36,48] adequately. From the QM-optimized structure, parameters to perform the molecular dynamics (MD) simulations were extracted from the general Amber force field (GAFF). The bond lengths, angles, and dihedral angles were calculated by using the parmcal program available in the AmberTools suit of programs as previously described [48]. To assess the interactions of the two copper compounds with a bilayer membrane, MD simulations were run with the compounds at two different starting positions (see Fig. S3 in the Supporting Information). Each compound was manually positioned at either the surface of the membrane or inserted into the geometric center of mass (COM) of the entire membrane system. A dioleoylphosphatidylcholine (DOPC) membrane model was constructed by using the AMBER Lipid 14 force field. The system was explicitly solvated by using the TIP3P water model in a periodic orthogonal box and neutralized with Na^+ ions. The Joung–Cheatham ion model [49] was used, and an excess of NaCl ions was added until a final concentration of 200 mM was reached. Minimization was performed for 2000 steps using positional restraints (harmonic constant value of 10 kcal Å–2) to ensure no atom-overlapping was present in the initial model. This was followed by 5 equilibration steps, each 1 ns long and decreasing in each step the value of the harmonic constant (from 5 to 0.5 kcal $Å^{-2}$) on the solute. A final equilibration step with no restraints was performed for 0.1 ns. Production simulations at 300 K were performed for 2.5 μs by using the GPU version of the pmemd simulation engine available in AMBER14 [50–52]. Analysis was performed by using version 15 of the cpptraj analysis tool [53]. Energy analysis was performed by using the MM-PBSA utility [54]. In addition to unbiased MD simulations and to understand the energetic analysis of the diffusion of the complexes through the membrane, biased sampling was used by means of umbrella sampling to construct a pathway of insertion through the membrane. This method consists of a series of intermediate steps along a predefined reaction coordinate that effectively samples an energy pathway with the aid of a biasing potential. Starting with the compound inserted at the center of mass of the bilayer membrane, a biasing force was imposed between the center of mass of the membrane and the center of mass of the compound. The sampling was carried out by increasing the distance from the COM of the membrane from 1 to 20 Å in increments of 1 Å. The resulting potential of mean force profile was constructed by using the weighted histogram analysis method (WHAM) [55,56].

Acknowledgments

The authors thank CONACyT Redes temáticas 294727 (Farmoquímicos), 293418(Red Internacional de Bionanotecnología) and UNAM-PAPIIT-IG200616 for the financial support. This work was supported by the Center for High Performance Computing at the University of Utah.

Appendix A. Supplementary data

Supplementary data to this article can be found online at https://doi.org/10.1016/j.jinorgbio.2019.03.012.

References

[1] L. Savioli, H. Smith, A. Thompson, Giardia and cryptosporidium join the “neglected diseases initiative”, Trends Parasitol. 22 (2006) 203–208, https://doi.org/10.1016/j.pt.2006.02.015.
[2] P.R. Torgerson, B. Devleesschauwer, N. Praet, N. Speybroeck, A.L. Willingham, F. Kasuga, M.B. Rokni, X.N. Zhou, E.M. Fèvre, B. Sripa, N. Gargouri, T. Fürst, C.M. Budke, H. Carabin, M.D. Kirk, F.J. Angulo, A. Havelaar, N. de Silva, World Health Organization estimates of the global and regional disease burden of 11 foodborne parasitic diseases, 2010: a data synthesis, PLoS Med. 12 (2015) 1–22, https://doi.org/10.1371/journal.pmed.1001920.
[3] R.C.A. Thompson, Giardiasis as a re-emerging infectious disease and its zoonotic potential, Int. J. Parasitol. 30 (2000) 1259–1267, https://doi.org/10.1016/S0020-7519(00)00127-2.
[4] A. Efstratiou, J.E. Ongerth, P. Karanis, Waterborne transmission of protozoan parasites: review of worldwide outbreaks - an update 2011–2016, Water Res. 114 (2017) 14–22, https://doi.org/10.1016/j.watres.2017.01.036.
[5] R. Cedillo-Rivera, Y.A. Leal, L. Yépez-Mulia, A. Gómez-Delgado, G. Ortega-Pierres, R. Tapia-Conyer, O. Muñoz, Seroepidemiology of giardiasis in Mexico, Am. J. Trop. Med. Hyg. 80 (2009) 6–10.
[6] D.S. Berkman, A.G. Lescano, R.H. Gillman, S.L. Lopez, M.M. Black, Effects of stunting, diarrhoeal disease, and parasitic infection, Lancet 359 (2002) 564–571 http://search.proquest.com/docview/199007689/fulltextPDF/7FB75FF7AD3E4269PQ/16?accountid=32506.
[7] C. Eppig, C.L. Fincher, R. Thornhill, Parasite prevalence and the worldwide distribution of cognitive ability, Proc. R. Soc. B Biol. Sci. 277 (2010) 3801–3808, https://doi.org/10.1098/rspb.2010.0973.
[8] R.D. Adam, Biology of Giardia lamblia, Clin. Microbiol. Rev. 14 (2001) 447–475, https://doi.org/10.1128/CMR.14.3.447-475.2001.
[9] B.R.E. Ansell, M.J. McConville, S.Y. Ma'ayeh, M.J. Dagley, R.B. Gasser, S.G. Svärd, A.R. Jex, Drug resistance in Giardia duodenalis, Biotechnol. Adv. 33 (2015) 888–901, https://doi.org/10.1016/j.biotechadv.2015.04.009.
[10] T.B. Gardner, D.R. Hill, Treatment of giardiasis, Clin. Microbiol. Rev. 14 (2001) 114–128, https://doi.org/10.1128/CMR.14.1.114-128.2001.
[11] J.C. Craft, T. Murphy, J.D. Nelson, Furazolidone and quinacrine. Comparative study

of therapy for giadiasis in children, Am. J. Dis. Child. 135 (1981) 164–166.
[12] L.J. Robertson, K. Hanevik, A.A. Escobedo, K. Mørch, N. Langeland, Giardiasis - why do the symptoms sometimes never stop? Trends Parasitol. 26 (2010) 75–82, https://doi.org/10.1016/j.pt.2009.11.010.
[13] A. Hall, Q. Nahar, Albendazole as a treatment for infections with giardia duodenalis in children in Bangladesh, Trans. R. Soc. Trop. Med. Hyg. 87 (1993) 84–86, https://doi.org/10.1016/0035-9203(93)90435-S.
[14] H.M. Gilles, P.S. Hoffman, Treatment of intestinal parasitic infections: a review of nitazoxanide, Trends Parasitol. 18 (2002) 95–97, https://doi.org/10.1016/S1471-4922(01)02205-X.
[15] S. Solaymani-Mohammadi, J.M. Genkinger, C.A. Loffredo, S.M. Singer, A meta-analysis of the effectiveness of albendazole compared with metronidazole as treatments for infections with Giardia duodenalis, PLoS Negl. Trop. Dis. 4 (2010), https://doi.org/10.1371/journal.pntd.0000682.
[16] J.M. Ordóñez-Mena, N.D. McCarthy, T.R. Fanshawe, Comparative efficacy of drugs for treating giardiasis: a systematic update of the literature and network meta-analysis of randomized clinical trials, J. Antimicrob. Chemother. 73 (2018) 596–606, https://doi.org/10.1093/jac/dkx430.
[17] N. Sangster, P. Batterham, H.D. Chapman, M. Duraisingh, L. Le Jambre, M. Shirley, J. Upcroft, P. Upcroft, Resistance to antiparasitic drugs: the role of molecular diagnosis, Int. J. Parasitol. 32 (2002) 637–653, https://doi.org/10.1016/S0020-7519(01)00365-4.
[18] L.E.B. Nabarro, R.A. Lever, M. Armstrong, P.L. Chiodini, Increased incidence of nitroimidazole-refractory giardiasis at the Hospital for Tropical Diseases, London: 2008-2013, Clin. Microbiol. Infect. 21 (2015) 791–796, https://doi.org/10.1016/j.cmi.2015.04.019.
[19] Y. Toledano-Magaña, J.C. García-Ramos, C. Torres-Gutiérrez, C. Vázquez-Gasser, J.M. Esquivel-Sánchez, M. Flores-Alamo, L. Ortiz-Frade, R. Galindo-Murillo, M. Nequiz, M. Gudiño-Zayas, J.P. Laclette, J.C. Carrero, L. Ruiz-Azuara, Water-soluble ruthenium (II) chiral heteroleptic complexes WITH Amoebicidal in vitro and in vivo activity, J. Med. Chem. 60 (2017) 899–912, https://doi.org/10.1021/acs.jmedchem.6b00795.
[20] C. Sarniguet, J. Toloza, M. Cipriani, M. Lapier, M. Vieites, Y. Toledano-Magaña, J.C. García-Ramos, L. Ruiz-Azuara, V. Moreno, J.D. Maya, C.O. Azar, D. Gambino, L. Otero, Water-soluble ruthenium complexes bearing activity against protozoan parasites, Biol. Trace Elem. Res. 159 (2014) 379–392, https://doi.org/10.1007/s12011-014-9964-0.
[21] J.C. García-Ramos, Y. Toledano-Magaña, L.G. Talavera-Contreras, M. Flores-Álamo, V. Ramírez-Delgado, E. Morales-León, L. Ortiz-Frade, A.G. Gutiérrez, A. Vázquez-Aguirre, C. Mejía, J.C. Carrero, J.P. Laclette, R. Moreno-Esparza, L. Ruiz-Azuara, Potential cytotoxic and amoebicide activity of first row transition metal compounds with 2,9-bis-(2′,5′-diazahexanyl)-1,1-phenanthroline (L1), Dalt. Trans. 41 (2012) 10164, , https://doi.org/10.1039/c2dt30224a.
[22] J.C. García-Ramos, A.G. Gutiérrez, A. Vázquez-Aguirre, Y. Toledano-Magaña, A.L. Alonso-Sáenz, V. Gómez-Vidales, M. Flores-Alamo, C. Mejía, L. Ruiz-Azuara, The mitochondrial apoptotic pathway is induced by Cu(II) antineoplastic compounds (Casiopeínas(R)) in SK-N-SH neuroblastoma cells after short exposure times, BioMetals 30 (2017) 43–58, https://doi.org/10.1007/s10534-016-9983-8.
[23] A.G. Gutiérrez, A. Vázquez-Aguirre, J.C. García-Ramos, M. Flores-Alamo, E. Hernández-Lemus, L. Ruiz-Azuara, C. Mejía, Copper(II) mixed chelate compounds induce apoptosis through reactive oxygen species in neuroblastoma cell line CHP-212, J. Inorg. Biochem. 126 (2013) 17–25, https://doi.org/10.1016/j.jinorgbio.2013.05.001.
[24] C. Santini, M. Pellei, V. Gandin, M. Porchia, F. Tisato, C. Marzano, Advances in copper complexes as anticancer agents, Chem. Rev. 114 (2014) 815–862, https://doi.org/10.1021/cr400135x.
[25] F. Carvallo-Chaigneau, C. Trejo-Solís, C. Gómez-Ruiz, E. Rodríguez-Aguilera, L. Macías-Rosales, E. Cortés-Barberena, C. Cedillo-Peláez, I. Gracia-Mora, L. Ruiz-Azuara, V. Madrid-Marina, F. Constantino-Casas, Casiopeina III-ia induces apoptosis in HCT-15 cells in vitro through caspase-dependent mechanisms and has antitumor effect in vivo, BioMetals 21 (2008) 17–28, https://doi.org/10.1007/s10534-007-9089-4.
[26] C. Trejo-Solís, G. Palencia, S. Zuñiga, A. Rodríguez-Ropon, L. Osorio-Rico, S. Torres Luvia, I. Gracia-Mora, L. Marquez-Rosado, A. Sánchez, M.E. Moreno-García, A. Cruz, M.E. Bravo-Gómez, L. Ruiz-Ramírez, S. Rodríquez-Enriquez, J. Sotelo, Cas Ilgly induces apoptosis in glioma C6 cells in vitro and in vivo through caspase-dependent and caspase-independent mechanisms, Neoplasia 7 (2005) 563–574, https://doi.org/10.1593/neo.04607.
[27] C. Trejo-Solís, D. Jimenez-Farfan, S. Rodriguez-Enriquez, F. Fernandez-Valverde, A. Cruz-Salgado, L. Ruiz-Azuara, J. Sotelo, Copper compound induces autophagy and apoptosis of glioma cells by reactive oxygen species and jnk activation, BMC Cancer 12 (2012), https://doi.org/10.1186/1471-2407-12-156.
[28] A.R. Barbosa, K.R. Caleffi-Ferracioli, C.Q.F. Leite, J.C. García-Ramos, Y. Toledano-Magaña, L. Ruiz-Azuara, V.L.D. Siqueira, F.R. Pavan, R.F. Cardoso, Potential of Casiopeínas® copper complexes and antituberculosis drug combination against mycobacterium tuberculosis, Chemotherapy 61 (2016) 249–255, https://doi.org/10.1159/000443496.
[29] L. Becco, A. Rodríguez, M.E. Bravo, M.J. Prieto, L. Ruiz-Azuara, B. Garat, V. Moreno, D. Gambino, New achievements on biological aspects of copper complexes Casiopeínas®: interaction with DNA and proteins and anti-Trypanosoma cruzi activity, J. Inorg. Biochem. 109 (2012) 49–56, https://doi.org/10.1016/j.jinorgbio.2012.01.010.
[30] L. Ruiz-Azuara, Procedimiento para la obtención de complejos metálicos como agentes anticancerígenos, S.18802 172248 (1993).
[31] L. Ruiz-Azuara, Process to Obtain New Mix Copper Aminoacidate from Methylate Phenanthroline Complexes to Be Used as Anticancerigenic Agents, 5,576,326, (1996).
[32] M.E. Bravo-Gómez, J.C. García-Ramos, I. Gracia-Mora, L. Ruiz-Azuara, Antiproliferative activity and QSAR study of copper(II) mixed chelate [Cu(N-N)(acetylacetonato)]NO3and [Cu(N-N)(glycinato)]NO3complexes, (Casiopeínas®), J. Inorg. Biochem. 103 (2009) 299–309, https://doi.org/10.1016/j.jinorgbio.2008.10.006.
[33] J.C. García-Ramos, R. Galindo-Murillo, A. Tovar-Tovar, A.L. Alonso-Saenz, V. Gómez-Vidales, M. Flores-Álamo, L. Ortiz-Frade, F. Cortes-Guzmán, R. Moreno-Esparza, A. Campero, L. Ruiz-Azuara, The π-back-bonding modulation and its impact in the electronic properties of Cu(II) antineoplastic compounds: an experimental and theoretical study, Chemistry 20 (2014) 13730–13741, https://doi.org/10.1002/chem.201402775.
[34] R. Kachadourian, H.M. Brechbuhl, L. Ruiz-Azuara, I. Gracia-Mora, B.J. Day, Casiopeína IIgly-induced oxidative stress and mitochondrial dysfunction in human lung cancer A549 and H157 cells, Toxicology 268 (2010) 176–183, https://doi.org/10.1016/j.tox.2009.12.010.
[35] R. Galindo-Murillo, J.C. García-Ramos, L. Ruiz-Azuara, T.E. Cheatham, F. Cortés-Guzmán, Intercalation processes of copper complexes in DNA, Nucleic Acids Res. 43 (2015) 5364–5376, https://doi.org/10.1093/nar/gkv467.
[36] R. Galindo-Murillo, L. Ruíz-Azuara, R. Moreno-Esparza, F. Cortés-Guzmán, Molecular recognition between DNA and a copper-based anticancer complex, Phys. Chem. Chem. Phys. 14 (2012) 15539, , https://doi.org/10.1039/c2cp42185b.
[37] A.I. Valencia-Cruz, L.I. Uribe-Figueroa, R. Galindo-Murillo, K. Baca-López, A.G. Gutiérrez, A. Vázquez-Aguirre, L. Ruiz-Azuara, E. Hernández-Lemus, C. Mejía, Whole genome gene expression analysis reveals Casiopeína-induced apoptosis pathways, PLoS One 8 (2013), https://doi.org/10.1371/journal.pone.0054664.
[38] J.-C. García-Ramos, R. Galindo-Murillo, F. Cortés-Guzmán, L. Ruiz-Azuara, Metal-based drug-DNA interactions, J. Mex. Chem. Soc. 57 (2013) 160–174.
[39] I.V. Shemarova, Signaling mechanisms of apoptosis-like programmed cell death in unicellular eukaryotes, Comp. Biochem. Physiol. - B Biochem. Mol. Biol. 155 (2010) 341–353, https://doi.org/10.1016/j.cbpb.2010.01.010.
[40] J.C. García-Ramos, G. Vértiz-Serrano, L. Macías-Rosales, R. Galindo-Murillo, Y. Toledano-Magaña, J.P. Bernal, F. Cortés-Guzmán, L. Ruiz-Azuara, Isomeric effect on the pharmacokinetic behavior of anticancer CuIIMixed chelate complexes: experimental and theoretical approach, Eur. J. Inorg. Chem. 2017 (2017) 1728–1736, https://doi.org/10.1002/ejic.201601199.
[41] E. Chabrière, M.H. Charon, A. Volbeda, L. Pieulle, E.C. Hatchikian, J.C. Fontecilla-Camps, Crystal structures of the key anaerobic enzyme pyruvate ferredoxin oxidoreductase free and in complex with pyruvate, Nat. Struct. Biol. 6 (1999) 182–190, https://doi.org/10.1038/5870.
[42] W. Buckel, R.K. Thauer, Energy conservation via electron bifurcating ferredoxin reduction and proton/Na+ translocating ferredoxin oxidation, Biochim. Biophys. Acta Bioenerg. 1827 (2013) 94–113, https://doi.org/10.1016/j.bbabio.2012.07.002.
[43] J. Samuelson, Why metronidazole is active against both bacteria and parasites, Antimicrob. Agents Chemother. 43 (1999) 1533–1541 (doi:0066-4804/99/$04.00+0).
[44] V.V. Emelyanov, A.V. Goldberg, Fermentation enzymes of Giardia intestinalis, pyruvate: ferredoxin oxidoreductase and hydrogenase, do not localize to its mitosomes, Microbiology 157 (2011) 1602–1611, https://doi.org/10.1099/mic.0.044784-0.
[45] G.M. Sheldrick, SHELXT - integrated space-group and crystal-structure determination, Acta Crystallogr. Sect. A Found. Crystallogr. 71 (2015) 3–8, https://doi.org/10.1107/S2053273314026370.
[46] G.M. Sheldrick, Crystal structure refinement with SHELXL, Acta Crystallogr. Sect. C Struct. Chem. 71 (2015) 3–8, https://doi.org/10.1107/S2053229614024218.
[47] L.J. Farrugia, WinGX suite for small-molecule single-crystal crystallography, J. Appl. Crystallogr. 32 (1999) 837–838, https://doi.org/10.1107/S0021889899006020.
[48] R. Galindo-Murillo, J. Hernandez-Lima, M. González-Rendón, F. Cortés-Guzmán, L. Ruíz-Azuara, R. Moreno-Esparza, π-Stacking between Casiopeinas® and DNA bases, Phys. Chem. Chem. Phys. 13 (2011) 14510–14515, https://doi.org/10.1039/c1cp20183b.
[49] I.S. Joung, T.E. Cheatham, Determination of alkali and halide monovalent ion parameters for use in explicitly solvated biomolecular simulations, J. Phys. Chem. B 112 (2008) 9020–9041, https://doi.org/10.1021/jp8001614.
[50] R. Salomon-Ferrer, A.W. Götz, D. Poole, S. Le Grand, R.C. Walker, Routine microsecond molecular dynamics simulations with AMBER on GPUs. 2. Explicit solvent particle mesh ewald, J. Chem. Theory Comput. 9 (2013) 3878–3888, https://doi.org/10.1021/ct400314y.
[51] A.W. Götz, M.J. Williamson, D. Xu, D. Poole, S. Le Grand, R.C. Walker, Routine microsecond molecular dynamics simulations with AMBER on GPUs. 1. Generalized born, J. Chem. Theory Comput. 8 (2012) 1542–1555, https://doi.org/10.1021/ct200909j.
[52] S. Le Grand, A.W. Götz, R.C. Walker, SPFP: speed without compromise - a mixed precision model for GPU accelerated molecular dynamics simulations, Comput. Phys. Commun. 184 (2013) 374–380, https://doi.org/10.1016/j.cpc.2012.09.022.
[53] D.R. Roe, T.E. Cheatham, PTRAJ and CPPTRAJ: software for processing and analysis of molecular dynamics trajectory data, J. Chem. Theory Comput. 9 (2013) 3084–3095, https://doi.org/10.1021/ct400341p.
[54] B.R. Miller, T.D. McGee, J.M. Swails, N. Homeyer, H. Gohlke, A.E. Roitberg, MMPBSA.py: an efficient program for end-state free energy calculations, J. Chem. Theory Comput. 8 (2012) 3314–3321, https://doi.org/10.1021/ct300418h.
[55] S. Kumar, J.M. Rosenberg, D. Bouzida, R.H. Swendsen, P.A. Kollman, THE weighted histogram analysis method for free-energy calculations on biomolecules. I. The method, J. Comput. Chem. 13 (1992) 1011–1021, https://doi.org/10.1002/jcc.540130812.
[56] T. Straatsma, Computational alchemy, Annu. Rev. Phys. Chem. 43 (1992) 407–435, https://doi.org/10.1146/annurev.physchem.43.1.407.